The Hydroclimatology of Kuwait: Explaining the Variability of Rainfall at Seasonal and Interannual Time Scales

Marc P. Marcella and Elfatih A. B. Eltahir

Massachusetts Institute of Technology, Cambridge, Massachusetts

(Manuscript received 13 August 2007, in final form 8 February 2008)

ABSTRACT

This paper presents an analysis of the spatial, seasonal, and interannual variabilities of Kuwaiti rainfall. Based on an analysis of rain gauge, as well as satellite, datasets, it is estimated that about 110–190 mm of rainfall occurs annually in Kuwait, depending on the dataset sampled. The corresponding estimates for the standard deviations of the annual rainfall are about 40–70 mm. Discrepancies between values arise from the different techniques used in constructing each dataset. Moreover, the spatial distribution of annual rainfall features a gradual increase from the southwest to the northeast. A distinct rainy season occurs from November to April, with double peaks in January and March. In addition, the seasonal variability of rainfall is associated with shifts in patterns of midlatitude storm tracks, which propagate southward toward the Middle East during the winter and spring season. These trends are characterized using estimates of the spatial correlations of rainfall in Kuwait with the surrounding region. At the interannual time scale, significant correlation is found between the tropical El Niño–Southern Oscillation (ENSO) and annual rainfall anomalies. Similar weak correlations are found between midlatitude rainfall in Europe and rainfall in Kuwait. The weak connections observed with both tropical and midlatitude atmospheric systems are consistent with the fact that Kuwait is located in the transitional zone between the tropics and midlatitudes.

1. Introduction

Surrounded by the Syrian and Arabian Deserts to the west and the Persian Gulf to the east, the country of Kuwait is located in a semiarid climate zone (see Fig. 1). The combination of short, distinct, rainy seasons and limited renewable freshwater resources is a strong motivation to study the variability of rainfall in this region. Furthermore, isolated heavy rainfall events can spur flash flooding and extensive property damage in urban areas such as Kuwait City (Al Kulaib 1984). Therefore, it is critical to have a firm understanding of the temporal and spatial distributions of rainfall in the country. To date, no prior studies have extensively described the hydroclimatology of Kuwait.

Here, a comprehensive and detailed rainfall history that includes traditional land measurements as well as novel satellite observations is compiled for the country and the surrounding region. From this dataset, the rainfall variability over Kuwait is described. Walters (1988) provides a thorough description of circulation patterns of the Middle East but mentions neither Kuwait's rainfall nor its climate in detail. In contrast, Al Kulaib (1984) describes the major climatic characteristics of the country but does not compile a complete rainfall record. Hence, for any future climate analysis or modeling, a reliable rainfall climatology must be constructed. Thus, with the use of rain gauges and satellite measurements, this study quantitatively details the variability of Kuwait's rainfall.

Finally, in an attempt to explain the variability of Kuwait's rainfall, these datasets are also used to test for correlations between the country's rainfall and other large-scale atmospheric circulation patterns spanning the globe. As a result, these findings should explain some of the rainfall variability in Kuwait. Given Kuwait's unique location in a transitional area between the tropics and midlatitudes, highlighting the contributions of both climate zones to Kuwait's rainfall provides a fundamental tool in discerning how sensitive the country and the surrounding region's rainfall is to large-scale climate change. For example, can changes in the

Corresponding author address: Marc Pace Marcella, Ralph M. Parsons Laboratory, Dept. of Civil and Environmental Engineering, Bldg. 48-305, MIT, 77 Massachusetts Ave., Cambridge, MA 02139.
E-mail: marcpace@mit.edu

DOI: 10.1175/2008JHM952.1

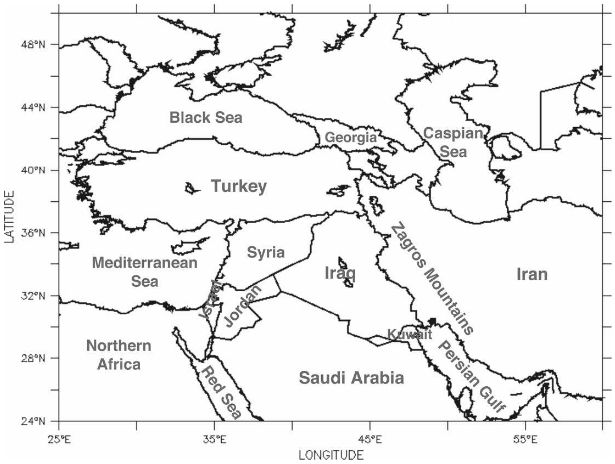

FIG. 1. Middle Eastern countries, major bodies of water, and geographic features relevant to this study.

strength of the North Atlantic Oscillation (NAO) greatly affect Kuwait's yearly rainfall? Or, do fluctuations in Pacific sea surface temperatures, such as El Niño events, dictate rainfall variability of the northern Arabian Peninsula? Essentially, do midlatitude or tropical climate features dictate this region's rainfall? Such are the type of questions posed in this work. As a result, this study should contribute toward a better understanding of the atmospheric phenomena responsible for shaping the hydroclimatology of the region.

2. Observational datasets

The country of Kuwait spans a small area from 28.4° to 30.2°N and from 46.5° to 48.5°E. Accordingly, datasets with a long historical record (more than 20 years) as well as high spatial resolution are desired. As a result, the following three datasets are used in the analysis. Table 1 provides a summary of the temporal coverage of each dataset.

a. Climate Research Unit high-resolution gridded dataset TS 2.1 (CRU)

The Climate Research Unit (CRU, located within the University of East Anglia, Norwich, United Kingdom) fine-resolution gridded dataset (TS 2.1) consists of a monthly time series of various climate variables covering the period 1900–2002. Such variables include surface temperature, precipitation, and vapor pressure—all interpolated from surface observations onto a global 0.5° × 0.5° resolution grid (Mitchell and Jones 2005). The goal of the CRU database is to provide the best estimate of the spatial pattern of climate variables at any moment in time (New et al. 1999). The weight placed on each station for a given grid box is a function of the station's distance from the grid box assuming an exponential correlation decay distance (450-km correlation scale for precipitation). If there is insufficient data for a grid box, the 1960–90 average value is used to compute the result. The exact construction and description of the interpolation scheme used for each variable can be found in Mitchell and Jones (2005). Station data come from a wide variety of sources [from World Meteorological Organization (WMO) stations to government agencies]; however, exact station information (i.e., location and record) is not available to the public domain. Moreover, it is important to note that the CRU dataset is land based only and sensitive to the details of the observational network in a certain region. Therefore, CRU totals are not available for the Persian Gulf or other major water bodies in the study region such as the Mediterranean and Black Seas. Likewise, CRU values over mountainous regions, where station coverage is scarce, may also be somewhat inaccurate.

TABLE 1. Summary of the Kuwaiti rainfall for the CRU, GPCP, and WMO datasets.

	CRU	GPCP	WMO
Temporal coverage	1952–2002	1979–2004	1961–2002
Annual rainfall μ (mm)	112	188	114
Std dev σ (mm)	39	72	67
Coefficient of variation C_v	0.35	0.38	0.59

The CRU data available for the past 50 yr (1952–2002) are used in this study. However, due to the lack of observations in this region, a large amount of smoothing may occur in CRU estimates of precipitation. For example, within the time period of the CRU data used in this study, only six stations, on average, are within the 450-km range of the target region. In fact, most of these stations are located to the north and east of Kuwait. For approximate locations of the mean climatology stations, the authors refer the reader to New et al. (1999). It is observed that during this time only one station is continuously located within the country of Kuwait, itself. Thus, with the rather coarse spatial contribution of the station data in Kuwait, this estimate may exclude convective, mesoscale rainfall that does occur in the country (Al Kulaib 1984). On the contrary, with contributions from stations farther north, the CRU estimates will include more rainfall that occurs from northerly large-scale systems that may not reach Kuwait. The implications of this methodology in constructing the CRU dataset will be discussed when comparing the dataset to the Global Precipitation Climatology Project (GPCP) results and the Kuwait International Airport station data in section 5.

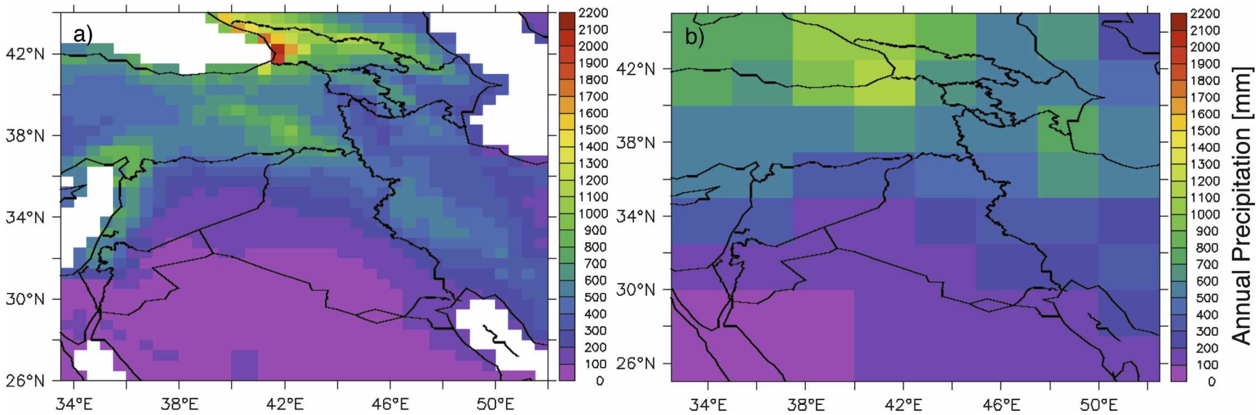

FIG. 2. Average annual precipitation (mm) for the Middle East for (a) the CRU dataset ranging from 1952 to 2002 and (b) the GPCP dataset ranging from 1979 to 2004.

b. Global Precipitation Climatology Project (GPCP)

Created in 1979 by the World Climate Research Program (WCRP), the GPCP combines satellite observations and station gauge measurements to provide rainfall estimates. Satellite measurements are computed from the Special Sensor Microwave Imager (SSM/I) as well as the Atmospheric Infrared Sounder (AIRS; Adler et al. 2003). Estimates obtained from the SSM/I and AIRS are then merged with rain gauge data, which are collected and maintained by the Global Precipitation Climatology Center (GPCC) of the National Climate Data Center (NCDC). The GPCC collects and analyzes station data from synoptic reports, climate summaries, and national collections. The output is a monthly, global, total precipitation product at 2.5° × 2.5° resolution from 1979 to the present. Since GPCP totals are derived from satellite measurements, the dataset does provide coverage over water bodies, which is lacking in the CRU dataset. However, the values from the project are significantly coarser than those of CRU's TS 2.1 (2.5° versus 0.5°). In addition, it is important to note that no single satellite data source encompasses the entire GPCP record and that there are four distinct periods in which data coverage changed, including the incorporation of SSM/I data in 1987.

Because GPCP data are based on satellite measurements of rainfall rather than ground measurements, the lack of subcloud evaporation in a semiarid region may be of significant importance. For example, the work of Marcella and Eltahir (2008) confirms the importance of subcloud evaporation in dictating the annual and interannual variability of Kuwait's rainfall. In addition, the work of Rosenfeld and Mintz (1988) suggests that, based on radar estimates, between 20% and 50% of rainfall can evaporate before reaching the surface in semiarid climates. As a result, even though GPCP satellite measurements are merged with rain gauge data, an overestimation of rainfall by GPCP is likely due to rainfall evaporation.

c. Kuwait International Airport rain gauge (WMO)

Rain gauge data from Kuwait City's International Airport (29.13°N, 47.58°E) is also used in the analysis. The Kuwait International Airport has kept a nearly continuous record of monthly mean temperature, pressure, and total precipitation from 1961 through 2002. Through the World Meteorological Organization (WMO) and the World Weather Records (WWR) compilation, this dataset is readily available. Other sources of station data within the country exist, but none with such a substantial continuity in coverage. Moreover, the airport data represent a point estimate and therefore cannot capture any of the spatial variability or localized rainfall occurring in other portions of the country. In addition, it is important to note station inhomogeneity that may have occurred at the airport. From urbanization in Kuwait City to changes in instrumentation, it is possible that the station data may have not been consistent for the past 50 yr (Peterson et al. 1998).

3. Rainfall statistics and variability

a. Spatial variability of annual rainfall

Shown in Figs. 2a and 2b are the spatial distributions of rainfall over the Middle East from both the CRU and GPCP datasets. Clear in both records is the gradient of precipitation that exists from the wetter regions in the north of the Black and Caspian Seas to the drier areas in the south of the Syrian Desert and Arabian Peninsula. Interestingly, the effects of orographic lifting

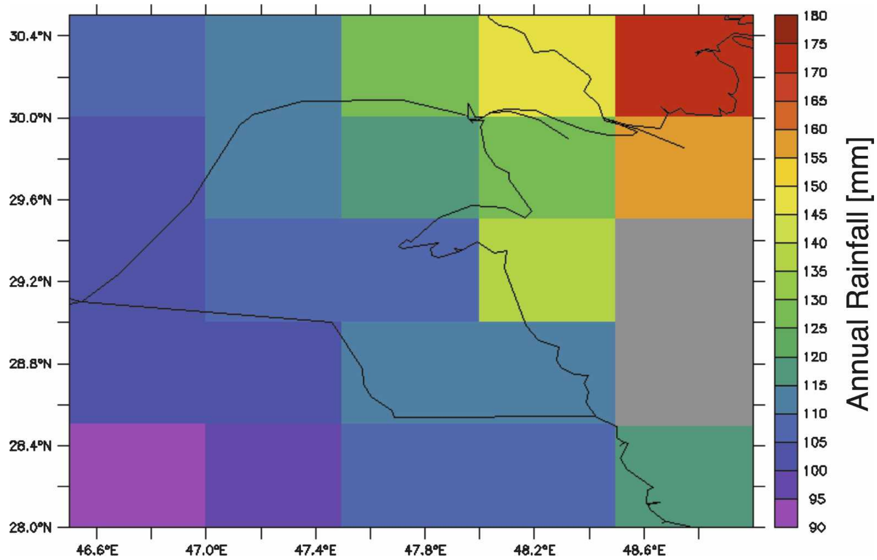

FIG. 3. Average annual rainfall (mm) for Kuwait based on the CRU 1952–2002 dataset. Since CRU features land-based estimates only, gray-shaded grid boxes denote missing data.

from the Zagros Mountains in western Iran are clearly seen where a northeast gradient of precipitation occurs over Kuwait, Iraq, and Iran. Although this pattern is noticeable in both the CRU and GPCP datasets, it is more apparent in the CRU data over Kuwait (Fig. 3). Here, nearly a doubling of the annual rainfall (from 90 to 180 mm) occurs from the southwest, bordering Saudi Arabia, to the northeast, near coastal southern Iran. Moreover, it appears that coastal areas of Kuwait exhibit higher annual totals than do interior regions (see Fig. 3). For example, rainfall totals increase from 100 mm in western Kuwait to nearly 140 mm along Kuwait's northeastern coastline. It is also apparent that while CRU is significantly wetter than GPCP in the Black Sea, Turkey, and Georgia regions, it is significantly drier in the southern areas of Iraq and northern Saudi Arabia (cf. Figs. 2a and 2b). The lack of a dense observational network may result in the CRU dataset failing to capture accurately the spatial distribution of rainfall in this southern area (Evans et al. 2004). Conversely, as mentioned previously, subcloud rainfall evaporation may result in GPCP significantly overestimating rainfall totals at the surface in this region. Thus, we believe the true rainfall totals lie in between the CRU and GPCP estimates.

The yearly average rainfall totals for Kuwait vary between the three datasets (see Table 1). Since Kuwait's rainy season occurs during the winter and spring months, the annual rainfall values presented are based on June–May totals. For example, the annual rainfall for 1987 is calculated by summing the rainfall from June 1987 to May 1988. While the CRU and WMO annual totals (112 and 114 mm, respectively) are similar, GPCP's value of 188 mm is nearly 67% more than the other two datasets. GPCP's larger totals are also visible in the time series shown in Fig. 4. In all but one year (1999), the GPCP yearly values are larger than CRU's. In fact, in above average rainfall years (i.e., 1992, 1994, 1995, and 1997), the GPCP values are nearly double those of CRU (see Fig. 4a). This trend is also visible at Kuwait City. In Fig. 4b, a comparison is made between the station data at Kuwait City airport (WMO) and the closest grid box in the GPCP and CRU datasets that corresponds to the Kuwait City airport. Note that the WMO estimates fall in between the GPCP and CRU values in wet years. For example, in 1992, GPCP measures 353 mm for Kuwait while CRU measures only 155 mm. However, WMO falls in between these two estimates at 234 mm. In the years before the advent of GPCP, the smoothing that occurs with the CRU data is also noticeable. That is, WMO values for dry (below average rainfall) and wet (above average rainfall) years are more extreme than those of CRU. For instance, in the dry year of 1976, WMO recorded 43 mm of rainfall while CRU had nearly double this total, at 73 mm. In contrast, the wet year of 1975 sees a WMO rainfall total of 260 mm while CRU's value is merely 190 mm (Fig. 4b).

b. Seasonal cycle and variability

Rainfall in Kuwait occurs in a relatively short, distinct, cool period during the winter months when synoptic-scale systems originating farther north reach the region. This study aims at describing the rainy period

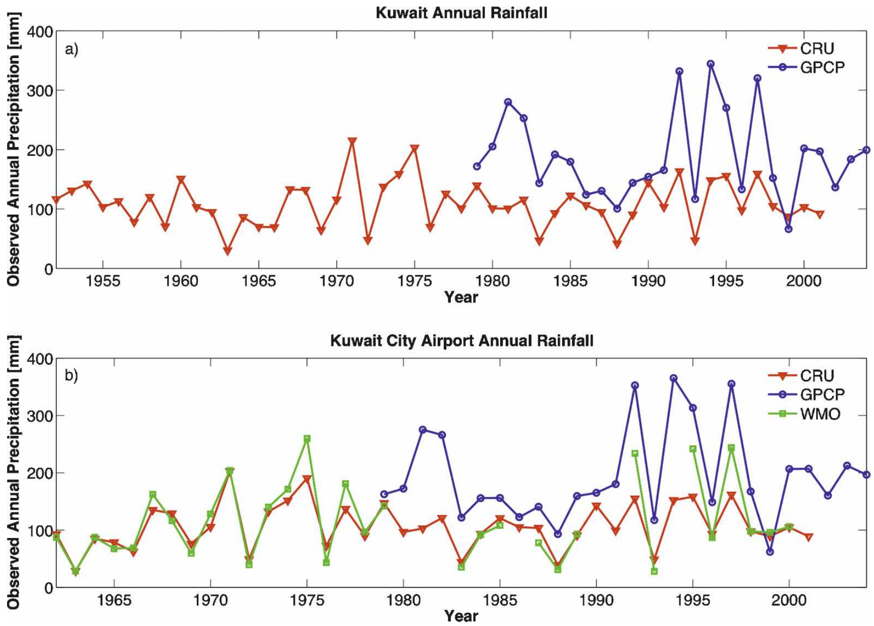

FIG. 4. Time series of annual rainfall (mm) from the CRU, GPCP, and WMO datasets for (a) the country of Kuwait and (b) Kuwait City International Airport. Note that grid boxes in CRU and GPCP containing the airport's location are used in (b).

using CRU, GPCP, and WMO data (Fig. 5). The seasonal cycles of the precipitation for all three datasets are remarkably similar. Some of this similarity is most likely due to the WMO rain gauges contributing to both the CRU averaging and GPCP merged values. Nevertheless, the onset of appreciable rainfall occurs in November and subsides by April. Although detectable rainfall usually begins in November and ends in April, Al Kulaib (1984) describes rare occasions in which rainfall occurs in October and May. This is evident in Fig. 5 with low average rainfalls but high standard deviations in these two months. In general, GPCP values are about 10 mm larger than either the CRU or WMO estimates in each month of the rainy season. Again, it is believed that the coarse resolution of GPCP, which includes wetter areas to the east in the Persian Gulf, as well as rainfall evaporation, results in estimates that are larger than the CRU and WMO values. Nevertheless, both the CRU and GPCP datasets have a dual peak in rainfall occurring in January and March, where 27 mm of rain falls in either month (averaged between the datasets).

Explaining the peaks of monthly rainfall in Kuwait requires an understanding of the cyclone climatology of the Middle East. Many studies have highlighted the dominant storms tracks of the eastern Mediterranean region where most of these systems develop. For example, Alpert et al. (2004) describe the southerly Red Sea trough (RST), which brings precipitation to Egypt, Israel, and the surrounding region via tropical moisture during the winter months. In such cases, these small disturbances produce only small amounts of precipitable water, which often evaporates in the arid, warm climates they traverse (Alpert et al. 2004). In contrast, the Syrian low (SL) track is characterized as a more northern pattern where a stronger, concentrated surface low pressure system forms off of the coast of Cyprus or Syria. This track results in larger, wetter storms that migrate southward toward the region (Kahana et al. 2002).

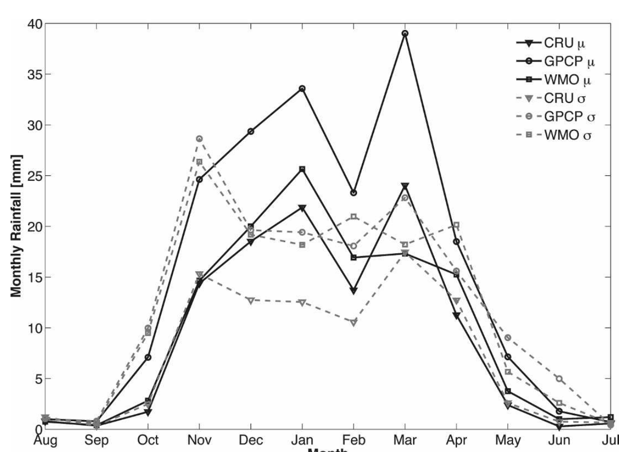

FIG. 5. Seasonal cycle of rainfall in Kuwait for the CRU and GPCP datasets and Kuwait City for WMO data. Monthly standard deviations are also plotted.

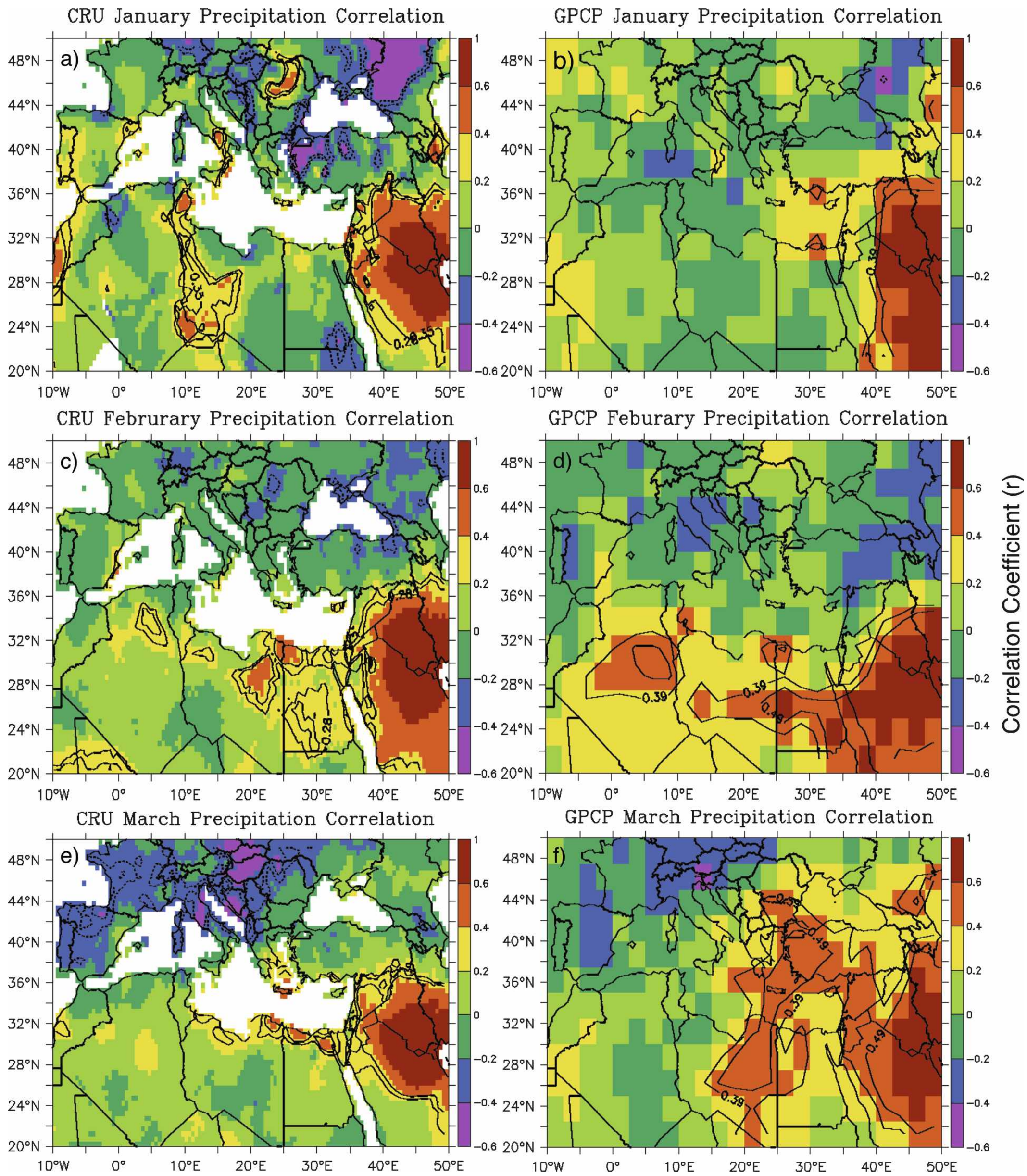

FIG. 6. Spatial correlation between Kuwaiti rainfall and surrounding precipitation for (a),(c),(e) CRU and (b),(d),(f) GPCP for the months of January, February, and March, respectively. Also contoured are the statistically significant correlation coefficients at the 95% and 99% confidence levels, which correspond to $r = \pm 0.28$ and $r = \pm 0.37$, respectively, for CRU, and $r = \pm 0.38$ and $r = \pm 0.49$, respectively, for GPCP.

It is these synoptic climatologies the can help explain the local minimum in February rainfall found in all three datasets. That is, the unique seasonal pattern of rainfall is most likely due to a shift in the predominant storm track position for Kuwait (see Fig. 6). During February, a more southerly storm track (from southern Egypt to the Red Sea and Saudi Arabia), the RST, becomes dominant over the region. Consequently, a reduction in the frequency of large-scale systems reaching the area from the stronger, wetter, northerly SL track (by Syria and Israel) occurs (Walters 1988). The SL track is noticeable in Figs. 6a and 6b, which show the high spatial correlation between Kuwaiti rainfall and rainfall in Syria and the eastern Mediterranean during the month of January. However, this connection decreases in February for both the CRU and GPCP datasets (cf. Fig. 6a to Fig. 6c and Fig. 6b to Fig. 6d). Here, a new pattern can be clearly seen in the high spatial correlation between February rainfall in Kuwait and northern Africa, namely Egypt and Libya (Figs. 6c

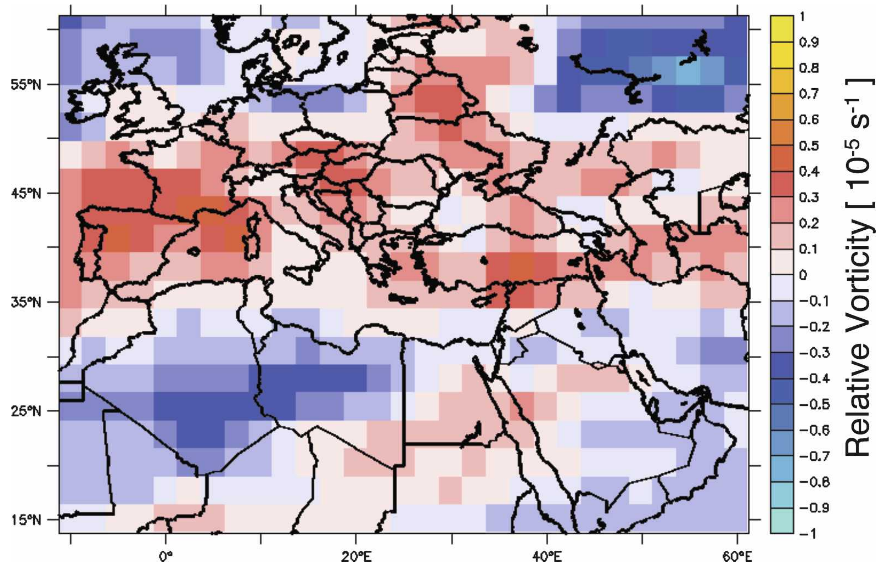

FIG. 7. Difference between ERA-40 average monthly values of the relative vorticity (10^{-5} s^{-1}) for the period of February minus January. These values are based on 46 yr of ERA-40 data (1957–2002).

and 6d). That is, in GPCP, a swath of statistically significant correlation (at the 99% confidence level) extends from Egypt across the Red Sea into eastern and central Saudi Arabia where correlation coefficients are above 0.50 (see Fig. 6d).

This feature also appears in the relative vorticity fields at 500 mb, a solid proxy for midlatitude disturbances. Using the 40-yr European Centre for Medium-Range Weather Forecasts (ECMWF) Re-Analysis (ERA-40) of Uppala et al. (2005), we compare the average monthly relative vorticity at 500 mb for the months of January and February. As seen in Fig. 7, an increase in relative vorticity occurs across southern Egypt and the Red Sea—the same location where the CRU and GPCP correlation values increase during February. This trend is also found in 500-mb geopotential heights (not shown) across the region, where a southward decrease in heights occurs. These patterns reveal a larger connection with rainfall from midlatitude disturbances that appear farther south in northern Africa and eastern Saudi Arabia during the month of February. Therefore, since the drier, less active RST pattern dominates in February, a reduction in rainfall is observed in Kuwait.

However, by March (Figs. 6e and 6f), the correlation between Kuwaiti rainfall and precipitation to the north by Syria and the eastern Mediterranean again increases; thus, Kuwaiti rainfall totals increase. In any event, it is important to note that all of these signals (precipitation correlations, vorticity differences, and geopotential height changes) are fairly weak. Such a weak signal is expected given that the absolute values of the monthly rainfall differences between January and February are only approximately 10 mm across all three datasets sampled—less than 10% of the total rainfall. In fact, WMO only slightly exhibits the dual-peak signature in March. Therefore, one should not expect a strong, pronounced difference but, rather, a weak yet spatially different pattern during February.

Finally, from Fig. 5 it can be seen that the months of November, March, and April have the largest standard deviations for monthly rainfall. When averaged over the three datasets, these values translate into the largest coefficients of variation occurring in November and April (1.34 and 1.1, respectively). Since these months mark the transitional periods of the rainy season, which, in itself, varies from year to year, this relatively large spread about the mean is expected.

c. Interannual and decadal variability

The combined characteristics of the different datasets mentioned above lead to a wide range of estimates of the interannual variability (see Table 1). As expected, CRU's standard deviation is lowest at 35 mm while GPCP is the highest at 72 mm, more than double that of CRU's. The airport data exhibit larger yearly variability than does CRU but less than GPCP at 67 mm. Moreover, the coefficient of variation, C_υ, is calculated to describe the dimensionless spread of the values about the mean. Here, the GPCP and CRU datasets have very similar values of C_υ at 0.38 and 0.35, respectively. However, the WMO data have a signifi-

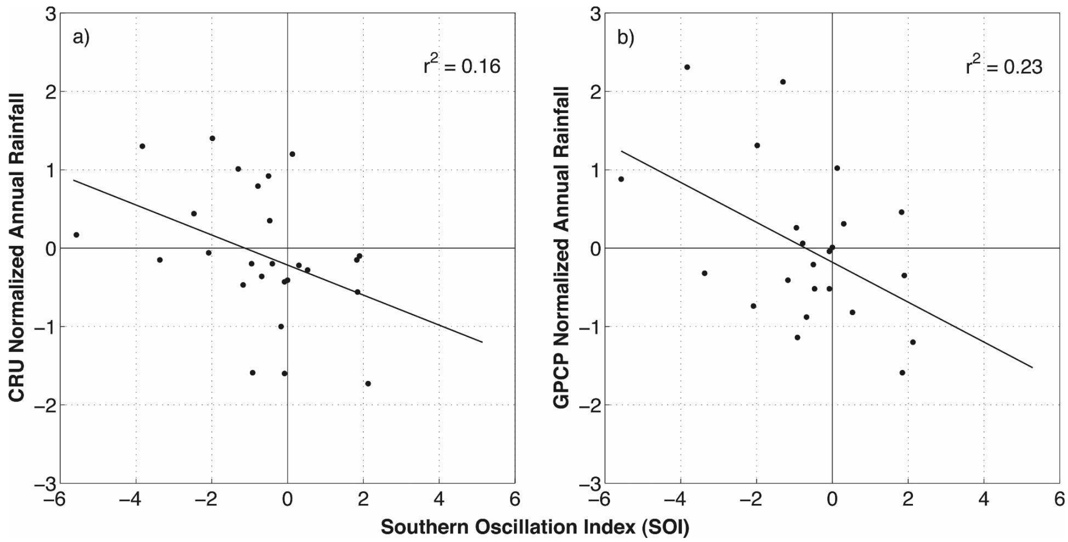

FIG. 8. Scatterplots showing the correlation between the average SOI for October–March and normalized annual rainfall anomalies in Kuwait from (a) CRU (1976–2001) and (b) GPCP (1979–2001). Also plotted are the best-fit lines and coefficient of determination (r^2).

cantly larger value at nearly 0.60. A larger coefficient of variation at Kuwait City Airport seems logical since no averaging of rain gauge data occurs, as is the case in the CRU and GPCP totals. In addition, as can be seen from the CRU data in Fig. 4, very little interdecadal variability occurs in the Kuwaiti rainfall. However, the lack of a consistent dataset that extends throughout the twentieth century makes analyzing the decadal variability of rainfall in Kuwait challenging.

4. Teleconnections with tropical and midlatitude atmospheric conditions

Much research has been done in studying the effects of large-scale atmospheric patterns such as the NAO (Hurrell 1995) and the El Niño–Southern Oscillation (ENSO; Kumar et al. 2006) on regional climates. For example, Cullen et al. (2002) examine the effects of the NAO teleconnection on streamflows of the Middle East at interannual and decadal time scales. However, here we investigate the relationship between Kuwait rainfall and NAO but find no significant correlation on a monthly or yearly time scale. These results are similar to those of Evans et al. (2004), who did not find a significant correlation between the NAO and rainfall in the Middle East.

Additionally, studies have shown that connections exist between ENSO anomalies and precipitation in Israel (Price et al. 1998). In a similar analysis, the correlation between the Southern Oscillation index (SOI) and normalized annual rainfall anomalies in Kuwait using both the CRU and GPCP datasets is completed (see Fig. 8). Our results indicate that there is a statistically significant negative relationship (at the 95% level) between the SOI and Kuwaiti rainfall in both datasets ($r = -0.40$ and $r = -0.48$, respectively). That is, in El Niño years (negative SOI indices), when Pacific Ocean sea surface temperature anomalies are positive, Kuwait's annual rainfall is above average. Nevertheless, the relationship is somewhat weak where only 16% of the variability in CRU annual rainfall can be explained by the ENSO phenomenon whereas 23% of the rainfall variability in GPCP is explained (Fig. 8). Interestingly, we find that this relationship extends only for the past 25 yr. A similar finding was reported by Price et al. (1998). Extending the analysis for longer time periods causes a significant decrease in the correlation between ENSO and Kuwaiti annual rainfall. Many studies (e.g., Rajagopalan et al. 1997; Wuethrich 1995) have documented changes in the frequency of El Niño events and the increased connection between Pacific and midlatitude ocean–atmosphere systems. These changes may explain the limited nature of the correlations observed between ENSO and Kuwaiti rainfall (Price et al. 1998).

Finally, the interannual variability of Kuwaiti rainfall can also be explained by the rainfall variability in the midlatitudes of Europe. More specifically, Fig. 9 displays the spatial correlation between Kuwaiti rainfall summed from November to April and the corresponding European and African rainfall in the CRU dataset. As seen in Fig. 9, a statistically significant negative correlation exists between rainfall in eastern Europe–

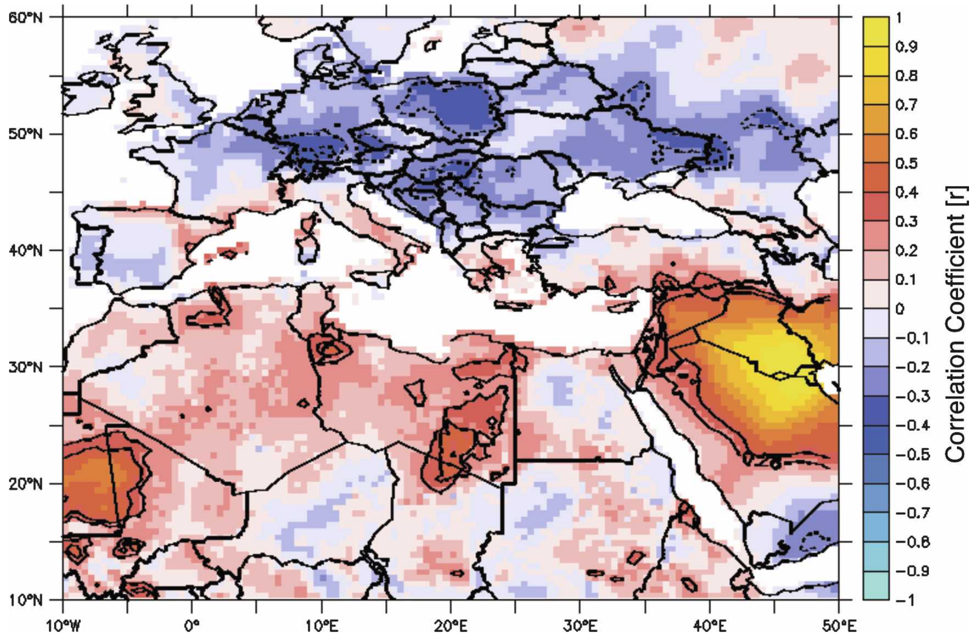

FIG. 9. Spatial correlation between CRU's Kuwait rainfall and surrounding precipitation for the November–April period. Note the contours for the statistically significant correlation coefficients at the 95% and 99% confidence levels, which correspond to $r = \pm 0.28$ and $r = \pm 0.37$, respectively.

Eurasia and rainfall in Kuwait during this period. In fact, a negative correlation between rainfall in this region and rainfall in Kuwait is also evident at the monthly time scale in both the CRU and GPCP datasets (Figs. 6a, 6c, and 6e). In contrast, a positive correlation between Kuwaiti rainfall and rainfall in northern Africa (the coastal areas of Algeria, Tunisia, and Libya) and the eastern Mediterranean is observed in Fig. 9. Likewise, this relationship between Kuwaiti rainfall and the rainfall of the eastern Mediterranean Sea is seen throughout the rainy season, notably in Figs. 6c and 6e. This positive correlation is most likely linked to cyclogenesis that takes place in the Mediterranean. The resulting storm systems migrate toward Kuwait causing much of the country's rainfall. It is important to mention that a similar analysis to that of Fig. 9 using the GPCP dataset does not reveal as clearly or strongly a correlation pattern as that of the CRU dataset.

In addition, the lack of correlation between precipitation in Israel–Lebanon and Kuwaiti rainfall needs some explanation. The lack of signal is due to the dominant wintertime precipitation processes over this region. It is known that the eastern coast of the Mediterranean Sea is characterized by steep mountainous topography, which causes seasonal upslope precipitation in Israel and Lebanon. In fact, over the area, the maximum winter precipitation (which is included in the period covered in this study's November–April correlation) is triggered by these coastal mountains (Evans et al. 2004). Thus, since this precipitation is more of a mesoscale, local phenomenon, one does not expect a correlation in this region to Kuwaiti rainfall. In fact, one may expect to see some dampening in the signal due to this mesoscale enhancing process, which is observed in Figs. 9 and 6a, 6c, and 6e.

5. Summary and conclusions

By compiling and comparing multiple datasets, the basic characteristics and statistics of Kuwait's rainfall are presented. Annual rainfall totals vary from 110 mm (CRU) to 190 mm (GPCP) for the country. In addition, all three datasets used here show the seasonal cycle of rainfall beginning in November, peaking in both January and March, and subsiding by April. Moreover, yearly standard deviations range from approximately 40 mm (CRU) to 70 mm (GPCP) while little interdecadal variability is observed.

Furthermore, the wide range in values from these observational datasets needs some explanation. Discrepancies between the CRU, GPCP, and WMO results arise from techniques used in creating both the CRU and GPCP datasets. In general, for above average rainfall years, the CRU totals are smaller than those of WMO. The airport's larger values are due to localized convective events occurring in the vicinity of the airport; these events are muted in the CRU averaging (Al Kulaib 1984). In contrast, in dry years, the WMO values are smaller than CRU's (see Fig. 4). In these years, convective activity is limited and rainfall is dominated by northerly large-scale depressions that traverse areas farther north. Therefore, CRU estimates, which have contributions from stations north of Kuwait (where a denser network of observations exists), overestimate the actual precipitation falling over Kuwait in such years. While both datasets have similar annual totals, WMO indicates a much larger standard deviation than CRU: 74 versus 40 mm (Table 1). This larger variation is expected from a point estimate or an individual station value such as the WMO dataset. As a result, the coefficient of variation for WMO is nearly 65% larger than that of CRU—thus revealing some of CRU's smoothing, which arises from averaging over multiple stations.

In contrast, GPCP mean estimates are consistently larger than either the CRU or WMO datasets. This difference is partly due to GPCP's coarse resolution and the use of satellite measurements for rainfall estimates. With a grid box of over 250 km in resolution, GPCP estimates rainfall over the wetter Persian Gulf and coastal Iran whereas CRU and WMO are land-based estimates at finer resolutions (56 km and point estimate, respectively.) In addition, as mentioned previously, satellite measurements neglect rainfall evaporation; consequently, the GPCP values may overestimate rainfall in semiarid regions such as Kuwait and Saudi Arabia. In any event, as seen in Fig. 4, when huge discrepancies do occur between CRU and GPCP, the WMO data consistently fall in between the other two datasets. Therefore, it is advantageous to include measurements from all three datasets.

The interannual variability of Kuwait rainfall is weakly influenced by both tropical (ENSO) and midlatitudinal (European rainfall) atmospheric features. Since Kuwait is located in the transitional zone between the tropics and the midlatitudes, rainfall in the country is expected to be connected to both tropical and midlatitudinal climates. Within the past 25 yr, Kuwait's annual rainfall anomalies are significantly correlated with the Southern Oscillation or El Niño phenomenon. The correlation explains 16% (CRU) or 23% (GPCP) of the interannual rainfall variability in Kuwait. Likewise, significant spatial correlations are found between Kuwait's rainfall and rainfall over Europe and the Mediterranean region. More specifically, Kuwait's annual rainfall (November–April) is found to be negatively correlated with corresponding Eurasian rainfall totals. On the other hand, regions of the Mediterranean and northern Africa are found to have positive correlations with Kuwait's annual rainfall. Finally, the seasonal variability in Kuwaiti rainfall is explained by the north–south migration of the dominant storm track over the region. That is, a positive correlation with rainfall over the eastern Mediterranean in January shifts farther south toward the Red Sea by February before moving north again toward Israel and Syria by March. Although most relationships between Kuwaiti rainfall and SOI indices (or rainfall patterns in Africa and Eurasia) are statistically significant, they are insufficient for forecasting Kuwait rainfall accurately.

The combined analysis presented here offers a comprehensive and concise description of Kuwaiti rainfall at both the seasonal and interannual time scales. Understanding more of the features that cause variability at these time scales may allow for the possibility of predicting the future variability of Kuwait's and the surrounding region's rainfall. For example, if confirmed that anthropogenic forcings do indeed cause an increase in both El Niño strength and frequency, then understanding the relationship between ENSO and Kuwaiti rainfall becomes particularly useful.

Acknowledgments. The authors are very grateful to all of the members of the Eltahir group and MIT Parsons Laboratory that contributed in some way to this work. Likewise, the authors thank two anonymous reviewers for their valuable insight and suggestions for improving this study. This work has been funded through support by the Kuwait Foundation for the Advancement of Science.

REFERENCES

Adler, R., and Coauthors, 2003: The Version 2 Global Precipitation Climatology Project (GPCP) monthly precipitation analysis (1979–present). *J. Hydrometeor.,* **4,** 1147–1167.

Al Kulaib, A., 1984: *The Climate of Kuwait.* Al Ressala P. Press, 178 pp.

Alpert, P., I. Osetnisky, B. Ziv, and H. Shafir, 2004: Semi-objective classification for daily synoptic systems: Application to the eastern Mediterranean climate change. *Int. J. Climatol.,* **24,** 1001–1011.

Cullen, H., A. Kaplan, P. Arkin, and P. B. Demenocal, 2002: Impact of the North Atlantic oscillation on Middle Eastern climate and streamflow. *Climatic Change,* **55,** 315–338.

Evans, J., R. Smith, and R. Oglesby, 2004: Middle East climate simulation and dominant precipitation processes. *Int. J. Climatol.,* **24,** 1671–1694.

Hurrell, J. W., 1995: Decadal trends in the North Atlantic oscillation: Regional temperature and precipitation. *Science,* **269,** 676–678.

Kahana, R., B. Ziv, Y. Enzel, and U. Dayan, 2002: Synoptic climatology of major floods in the Negev Desert, Israel. *Int. J. Climatol.,* **22,** 867–882.

Kumar, K. K., B. Rajagopalan, M. Hoerling, G. Bates, and M.

Cane, 2006: Unraveling the mystery of Indian monsoon failure during El Nino. *Science,* **314,** 115–118.

Marcella, M. P., and E. A. B. Eltahir, 2008: Modeling the hydroclimatology of Kuwait: The role of subcloud evaporation in semiarid climates. *J. Climate,* **21,** 2976–2989.

Mitchell, T. D., and P. D. J. Jones, 2005: An improved method of constructing a database of monthly climate observations and associated high-resolution grids. *Int. J. Climatol.,* **25,** 693–712.

New, M., M. Hulme, and P. Jones, 1999: Representing twentieth-century space–time climate variability. Part I: Development of a 1961–90 mean monthly terrestrial climatology. *J. Climate,* **12,** 829–856.

Peterson, T., and Coauthors, 1998: Homogeneity adjustments of in situ atmospheric climate data: A review. *Int. J. Climatol.,* **18,** 1493–1517.

Price, C., L. Stone, A. Huppert, B. Rajagopalan, and P. Alpert, 1998: A possible link between El Nino and precipitation in Israel. *Geophys. Res. Lett.,* **25,** 3963–3966.

Rajagopalan, B., U. Lall, and M. Cane, 1997: Anomalous ENSO occurrences: An alternate view. *J. Climate,* **10,** 2351–2357.

Rosenfeld, D., and Y. Mintz, 1988: Evaporation of rain falling from convective clouds as derived from radar measurements. *J. Appl. Meteor.,* **27,** 209–215.

Uppala, S., and Coauthors, 2005: The ERA-40 Re-analysis. *Quart. J. Roy. Meteor. Soc.,* **131,** 2961–3012.

Walters, K. R., 1988: The Persian Gulf region: A Climatological Study. Tech. Note USAFETAC/TN-88/002, USAF Environmental Technical Applications Center, Scott AFB, IL, 62 pp.

Wuethrich, B., 1995: El Niño goes critical. *New Scientist,* No. 1977, Reed Business Information, 32–35.